

SYNTHESIS, CHARACTERIZATION, DFT MODELING AND *IN VITRO* ANTIMYCOBACTERIAL ACTIVITY ASSAYS OF A SILVER(I)-ISONIAZID COMPLEX

José Alberto Paris Junior^a, Maurício Cavicchioli^{b,*}, Rachel Temperani Amaral Machado^c, Fernando Rogério Pavan^c, Douglas Hideki Nakahata^d, Pedro Paulo Corbi^d, Adão Marcos Ferreira Costa^e, Douglas Henrique Pereira^e and Antonio Carlos Massabni^a

^aUniversidade de Araraquara, 14801-320 Araraquara – SP, Brasil

^bDepartamento de Química Analítica, Físico-Química e Inorgânica, Instituto de Química, Universidade Estadual Paulista “Júlio de Mesquita Filho”, 14800-900 Araraquara – SP, Brasil

^cDepartamento de Ciências Biológicas, Faculdade de Ciências Farmacêuticas, Universidade Estadual Paulista “Júlio de Mesquita Filho”, 14800-903 Araraquara – SP, Brasil

^dInstituto de Química, Universidade Estadual de Campinas, 13083-970 Campinas – SP, Brasil

^eUniversidade Federal do Tocantins, Campus Gurupi, Gurupi – TO, Brasil

Recebido em 22/07/2020; aceito em 03/11/2020; publicado na web em 01/12/2020

In the present work, a silver(I) complex with the antimycobacterial drug isoniazid (inh) is described. Elemental and thermogravimetric analyses confirmed a 1:1 metal:ligand ratio for the silver-isoniazid (Ag-inh) complex with molecular composition $\text{AgC}_6\text{H}_7\text{N}_3\text{O}\cdot\text{NO}_3$. Infrared (IR) analysis suggests a bidentate coordination of isoniazid to silver by the nitrogen of the NH_2 group and by the oxygen of the $\text{C}=\text{O}$ group, and also confirms the presence of free nitrate anion. Coordination by the NH_2 group was reinforced by NMR measurements. Computational simulations using the density functional theory (DFT) reinforced that the ligand coordinates to the silver atom by the NH_2 and $\text{C}=\text{O}$ groups. The silver complex presented a minimal inhibitory concentration (MIC_{90}) of 0.78 $\mu\text{g}/\text{mL}$ against the standard *Mycobacterium tuberculosis* strain H37Rv. The data reported herein warrants further investigation on Ag-inh complex as a potential agent against tuberculosis.

Keywords: metallodrugs; bioinorganic chemistry; molecular modeling; *Mycobacterium tuberculosis*; antibacterial assays.

INTRODUCTION

There are about 1.5 million deaths annually due to tuberculosis (TB), which remains as a remarkable public health issue, causing concern worldwide. Globally, the best estimate is that 10 million people (range 9.0-11.1 million) developed TB in 2018: 57% of all TB cases are diagnosed in men, 32% in women and 11% in children.¹ The number of infections is growing up, especially in immunosuppressed patients (HIV), and in individuals with diabetes or receiving antitumor drugs.

Despite the improvement of TB treatment, it is severely affected by the appearance of multidrug-resistant *Mycobacterium tuberculosis* strains.² According to the World Health Organization Global Tuberculosis Report,¹ the best worldwide estimate is that, in 2018, about half a million people have developed TB resistance to rifampicin (RR-TB), the most effective first-line anti-TB drug. More alarming is that, within this group, 78% developed multidrug-resistant TB (MDR-TB). So, urgent actions are required to improve the coverage and quality of diagnosis, treatment and care for people with drug-resistant TB. These actions include the search of new drugs.³

Modification of old drugs is a strategy that can improve bioavailability and tolerability, which can decrease the resistance of pathogenic strains.⁴ Coordination of metal ions to drugs is a way to modify their chemical characteristics and consequently modify their pharmacokinetics, pharmacodynamics and mechanism of action on the bacteria.^{5,6}

Isoniazid (Figure 1), also called isonicotinic acid hydrazide (inh), was discovered in 1912, but its anti-TB activity was only reported on 1951. It belongs to the group of drugs called “first-line antimycobacterial

drugs”, which includes rifampicin (RIF), pyrazinamide (PZA) and ethambutol (ETH). The molecule has a heterocyclic N-atom of the pyridine ring and O- and N-atoms of the hydrazide group. Such coordination sites make inh an interesting ligand from the viewpoint of coordination chemistry.

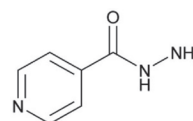


Figure 1. Structural formula of isoniazid (inh)

There are some reports of the synthesis of metal complexes with isoniazid in the literature. Cobalt and copper complexes with isoniazid were prepared by Hanson and Poggi.⁷ Their studies suggest that the metal is coordinated to inh by the nitrogen atom of the NH_2 group and the oxygen atom of the carbonyl group. Diniz et al. described a zinc(II) complex bound to two inh molecules, which also contains six hydration water molecules and two perchlorate counter-ions for each metal center. Zinc(II) adopts a distorted octahedral geometry, where two inh molecules is coordinated in a bidentate manner by the hydrazide group (N, O) and the other two inh residues complete the coordination sphere of zinc(II) binding to the aromatic nitrogen atoms.⁸ The authors also described mixed ligand complexes of Co(II), Zn(II) and Mg(II) containing inh as one of the ligands.^{9,10} Both complexes are coordination polymers.

Silver complexes and nanoparticles have also been considered in the search for novel active compounds against bacteria. Silver and several of its compounds have long been used as antimicrobial agents in medicine.¹¹⁻¹⁶ The Ag(I) sulfadiazine complex, for instance, has been used clinically as an antibacterial and antifungal agent since the

*e-mail: mauriciocavicchioli@gmail.com

1960s. It is an insoluble polymeric compound that slowly releases Ag(I) ions and is applied topically as a cream to prevent bacterial infections in cases of severe burns.^{11–14,17}

Initially, some studies have suggested that the primary target for inhibition of bacterial and yeast growth by silver(I) complexes is due to their binding to proteins containing S-donor ligands, and not nucleic acids as N/O donors.^{13,18,19} So, silver(I) complexes with N- and O-donor molecules have increased the ability to replace such molecules by the S-donor ligands of target bacterial proteins. Recently, it has been shown that silver ions target glyceraldehyde-3-phosphate dehydrogenase of the glycolytic pathway in *E. coli*, binding to cysteine and histidine residues in an almost linear geometry.²⁰ The most recent and broader investigation was done by H. Wang *et al.*²¹ The combined data from metalloproteomics and metabolomics indicated that Ag⁺ exerts its antimicrobial activity against *E. coli* by targeting important metabolic and physiological pathways. Primarily, Ag⁺ damages multiple enzymes in glycolysis and tricarboxylic acid (TCA) cycle, leading to the stalling of the oxidative branch of the TCA cycle and an adaptive metabolic divergence to the reductive glyoxylate pathway. This further damages the adaptive glyoxylate pathway and suppresses the cellular oxidative stress responses, causing systemic damages and death of the bacterium. As an example of these modifications, the levels of adenosine monophosphate (AMP), inosine-5'-monophosphate (IMP), hypoxanthine, guanosine, and uridine, which are involved in nucleic acid degradation or synthesis, decreased after Ag⁺ exposure.

The activity of silver complexes and formulations over tuberculosis is an emerging and promising field of research. Strong antimycobacterial activity against multi-drug-resistant *M. tuberculosis* of silver-carrying photocatalyst products was verified by Matsui *et al.*²² The development of strategies to modify an old drug and/or the combination of consolidated drugs, such as antibiotics, with metal ions with already known antimicrobial activities can lead to new and improved antibacterial agents. More recently, silver(I) complexes of fluoroanthranilic acid isomers were described in the literature and showed minimal inhibitory concentration (MIC₉₀) values around 10 μmol L⁻¹ against *M. tuberculosis* H37Rv bacterial strain, which are lower than the MIC₉₀ observed for the free ligands and silver nitrate.²³

Although no silver(I)-isoniazid complexes have been reported in the literature, a recent study showed that an inh and silver nitrate mixture with no isolation of the complex has a potent bactericidal effect on isoniazid-resistant clinical *M. tuberculosis* strains, resulting in lower MIC values than those from the isolate components. The authors claimed that the increased activity may be a result from an additive activity due to the increased production of reactive oxygen species by the combination treatment, which leads to oxidative stress and bacterial cell death.²⁴

In the present work a silver(I) complex with the first-line antimycobacterial drug isoniazid is described. The complex was synthesized, isolated and characterized by spectroscopic techniques and density functional theory (DFT) calculations, and its antimycobacterial properties were evaluated against the standard *Mycobacterium tuberculosis* strain H37Rv.

EXPERIMENTAL

Materials

Isoniazid and silver(I) nitrate were analytical grade products from Sigma/Aldrich chemical company. All other chemicals are analytical grade products from different sources. The reagents were used as received.

Synthesis

The silver complex with isoniazid was prepared by the addition of 10 mL of an aqueous solution containing 0.850 g (5.0 mmol) of silver(I) nitrate to 10 mL of an aqueous solution containing 0.685 g (5.0 mmol) of isoniazid under stirring in a dark room. Initially the solution changed to white and then a brownish precipitate was formed. The solid was collected by filtration, washed with water and left to dry in a desiccator with P₄O₁₀ in a dark room. Anal. Calc. for [Ag(C₆H₇N₃O)]·NO₃ (%), C 23.5, H 2.3, N 18.3. Found (%) C 22.8, H 1.73, N 18.8. No single crystals were obtained to perform a full X-ray crystallographic study.

Instrumental methods

Elemental analyses of carbon, hydrogen and nitrogen were performed using a CHNS-O 2400 series II (Perkin Elmer) Analyzer. High purity cysteine was used as a reference substance. Infrared (IR) spectra were recorded on a FT-IR Cary 630 Agilent Spectrophotometer, equipped with attenuated total reflectance (ATR) sampling apparatus. The resolution was set at 4 cm⁻¹. Thermal analysis was performed on a Thermoanalyzer TG/DTA simultaneous SDT Q-600 TA Instruments under the following conditions: α-alumina crucible, synthetic air (100 mL/min), heating rate of 10 °C per min, from 30 to 1000 °C. Solution-state ¹H and ¹³C nuclear magnetic resonance (NMR) spectra for free inh and its silver complex were recorded on Bruker AVANCE III 400 and 500 MHz spectrometers. The NMR spectra were acquired in deuterated dimethyl sulfoxide (dmsd-*d*₆) solutions and chemical shifts were given relative to tetramethylsilane (TMS).

Anti-Myco-bacterium tuberculosis analysis

Resazurin microtiter assay (REMA) was used to determine the MIC₉₀ of compounds against the standard *Mycobacterium tuberculosis* strain H37Rv. Briefly, the compounds were diluted in Middlebrook 7H9 broth, supplemented with OADC, and 0.5% glycerol. The solutions, in a range concentration of 0.09 to 25 μg mL⁻¹, were added to a 96-well microplate with the bacterial inoculum, adjusted to 10⁵ CFU mL⁻¹. The plates were incubated for 7 days at 37 °C, 5.0% CO₂ atmosphere. A solution of Resazurin was added at 0.01% in water and after incubation of 24 h, the fluorescence was read at 530/590 nm. Three biological replicates were performed. The MIC₉₀ was defined as the lowest concentration of compound able to inhibit 90% of mycobacterial growth.²⁵

Computational simulations

The density functional theory (DFT) was used to study the ligand and the silver complex. The possible structures of isoniazid and the Ag-inh complex [Ag(C₆H₇N₃O)]NO₃ were optimized to the minimum of energy with the hybrid functional B3LYP.^{26–29} The 6-31+G(d,p)^{30,31} basis sets were used for C, H, N and O atoms. For the Ag-atom, the LANL2DZ³² effective core potential basis set was used. Vibrational frequencies were calculated, and no imaginary frequencies were found, showing that the structures were at their minimum energy. All calculations were performed using the software Gaussian 09.³³ The topological analyses of the complexes were performed using the quantum theory of atoms in molecules (QTAIM)^{34,35} at the B3LYP/6-31+G(d,p)/LANL2DZ level. The QTAIM allows to characterize the chemical bond of the metal with the ligand and also to understand the nature of the bond. The QTAIM analyses were performed using the AIMALL package.³⁶

RESULTS AND DISCUSSION

Infrared spectroscopic analysis

The IR spectra of inh and the silver complex are presented in Figure 2. The main IR frequencies in the region 3500-600 cm^{-1} are shown in Table 1. The IR of inh is in accordance with the literature.³⁷

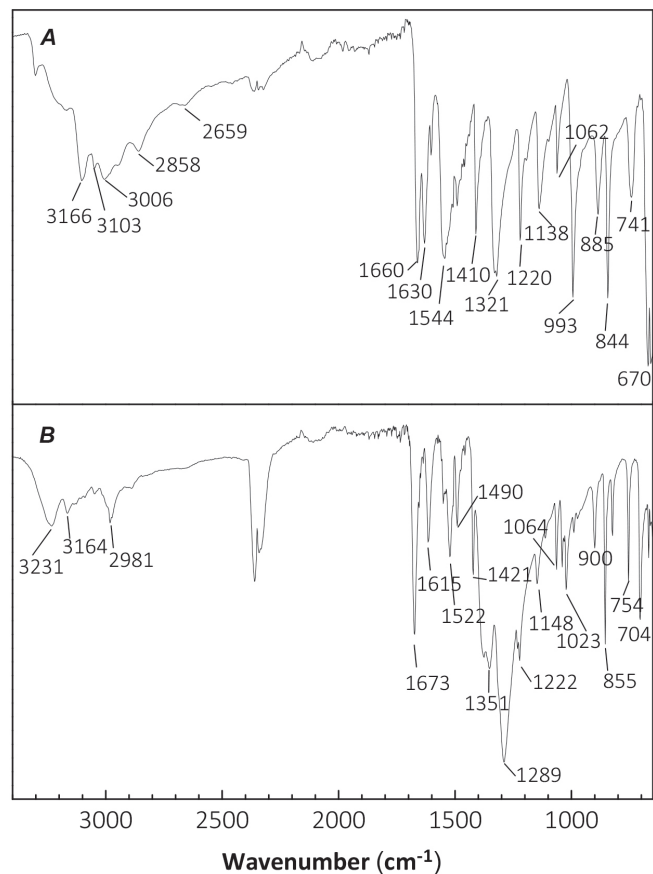


Figure 2. Infrared spectra of A) isoniazid (inh) and B) Ag-inh

Several IR bands of isoniazid had their frequencies changed after coordination to Ag(I). Among them, the band related to NH_2 wagging at 1630 cm^{-1} shifted to 1615 cm^{-1} in the complex and the band related to C=O at 1660 cm^{-1} was shifted to 1673 cm^{-1} in the complex. The changes observed when the IR spectra of the ligand and the Ag-inh complex are compared suggest coordination of the ligand to the metal by the nitrogen atom of the NH_2 group and also coordination by the oxygen atom of the C=O group.³⁸

Regarding the $\nu(\text{C-N})$ amide-like and the $\nu(\text{N-N})$ bands, a similar behavior was observed for the Co-inh complex early reported in the literature. The coordination affects only the amide-like stretching mode. Finally, the strong band at 1289 cm^{-1} in the spectrum of the metal complex confirms the presence of free NO_3^- as a counterion.³⁹

Thermogravimetric measurements

Figure 3 shows the thermogravimetric curve for the Ag-inh complex, with three well defined weight losses. The first loss of about 38% occurs in the range 140-200 °C. The other two mass losses occur in the ranges 200-280 °C and 320-360 °C which correspond to the decomposition of the ligand and the NO_3^- anion. The thermogravimetric curve shows a net weight loss of about 62%, with a final residue of 38%, which is consistent with the formation of Ag^0 .

Table 1. Main IR frequencies (cm^{-1}) of inh and the Ag-inh complex

isoniazid (inh)	Ag-inh complex	Vibrational assignments
670	704	$\tau(\text{C-C-C})_{\text{ring}} + \tau(\text{C-N-C-C})_{\text{ring}}$
741	754	δ ring
844	855	$\gamma(\text{C-C-H})$
885	900	$\gamma(\text{C-C-H})_{\text{ring}}; \delta(\text{C=O})$
993	1023	$\gamma(\text{C-C-H}); \gamma(\text{NH}_2)$
1062	1064	δ ring
1138	1148	$\nu(\text{N-N-H})_s$
1220	1222	$\delta(\text{C-H})$
	1289	νNO_3
1321	1351	$\nu(\text{C-N})_{\text{amide}}, \delta(\text{NH}_2)$
1410	1422	ν ring
1485	1490	ν ring
1545	1523	ν ring; wN-N-H
1630	1615	w NH_2
1660	1673	$\nu(\text{C=O})$
3000-3100	3000-3100	$\nu(\text{C-H})$
3166	3164	$\nu(\text{NH})$
3303	3223	$\nu(\text{NH}_2)$

ν : stretching; β : in plane bending; γ : out of plane bending; S: scissoring; τ : torsion; w: wagging.

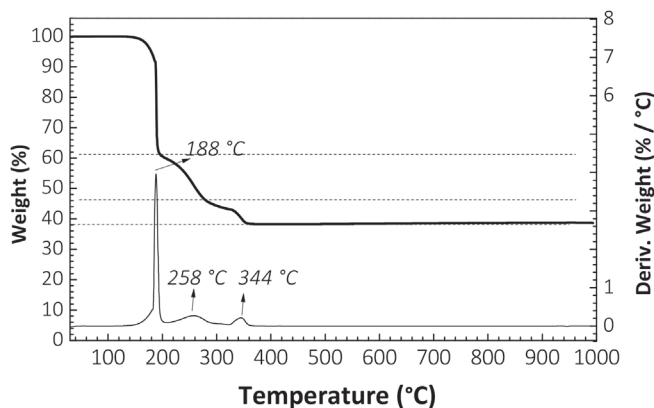


Figure 3. Thermogravimetric curves (TG and DTG) of the Ag-inh complex

Differential scanning calorimetry (DSC) analysis of the Ag-inh complex (see Figure 1S, Supplementary Material) indicates the occurrence of three exothermic events with their maxima at 190, 275 and at 348 °C, which correspond likely to oxidation of the ligand leading to the formation of silver residue.

Nuclear magnetic resonance spectroscopy

The ^1H and ^{13}C NMR spectra of the silver complex were evaluated in comparison to the spectra of free isoniazid to confirm the coordination sites of the ligand to the metal as suggested by the IR data.

The ^1H NMR spectra of inh and its Ag complex are presented in Figure 4 together with the numbered ligand structure. The most notable change in the spectrum of the metal complex when compared to the spectrum of the ligand is the signal from the hydrogen atoms of the NH_2 group (numbered as H7). The spectrum of the ligand shows a sharp signal at 4.64 ppm for the H-atoms of the NH_2 group. Upon

coordination, the same H-atoms are detected as a broad signal shifted downfield, with its maximum at 5.59 ppm ($\Delta\delta$ 0.95). In addition, the H-atom of the N-H group (H6) bonded to the NH_2 is also shifted downfield by 0.31 ppm, which reinforces the coordination of the NH_2 group of inh to Ag(I).

The analysis of the ^{13}C NMR spectra of inh and its silver complex (Figure 1S, Supplementary Material) did not permit us to confirm coordination of the ligand to silver by the O atom of the carbonyl group as first suggested by the IR data. No significant isomer shifts were detected when comparing the signal of the C atom of the carbonyl group in the ligand at 163.88 ppm with the same C atom in the complex, which was observed at 164.05 ppm. Also, the absence of significant changes in the signals of carbon atoms $\text{C}_{2,2'}$, $\text{C}_{3,3'}$ or C_4 (see Figure 1S, Supplementary Material) led us to discard N coordination of the pyridine ring of inh to Ag.

Nevertheless, considering that the infrared spectroscopic data suggested nitrogen of the NH_2 group and also oxygen coordination of the $\text{C}=\text{O}$ group to silver and that this coordination mode was already observed for a Cu(II) complex with inh, further studies based on DFT (see next section) were applied to evaluate if this bidentate coordination mode would in fact exist and if it would be the most stable one.

Molecular modeling

Due to the absence of crystals of the Ag-inh complex to perform a detailed X-ray crystallographic study and considering the possible coordination sites of inh to Ag suggested by IR and NMR spectroscopic measurements, DFT studies were performed to evaluate some possibilities of complexation. Such possibilities evaluated were calculated according to Figure 5.

Analyzing the theoretical results of four possible complexation sites, it is possible to infer that the structure where ligand coordination to Ag atom occurs by the N atom of the NH_2 group and oxygen atom of the group $\text{C}=\text{O}$ (Figure 5d) is the most stable one. The ligand coordination to Ag atom only by the nitrogen of the NH_2 group, Figure 5a, is the second most stable structure. The difference in the stability between metal complexes (Figure 5d and 5a) is small and on the order of 1.3 kcal mol $^{-1}$. On the other hand, the structure proposed on Figure 5b, where coordination was suggested to occur by the NH and NH_2 groups, shows that after the optimization of geometry the structure converges to the first hypothesis (Figure 5a). Finally, analyzing the complexation by the NH group (Figure 5c), it is possible to identify that the interaction occurs, but this is less stable because there is a steric hindrance for the ligand coordination to silver by the NH group. The difference in stability of complex (Figure 5c) in relation to the most stable complex is 11.16 kcal mol $^{-1}$ and in relation to the complex represented in Figure 5a the difference is 9.86 kcal mol $^{-1}$.

After determining the most stable structure, it is possible to analyze properties of the complex such as the optimal bond lengths N-Ag and O-Ag which were 2.60 and 2.30 Å, respectively. The coordination mode of inh to Ag(I) is the same observed for the Cu(II) complex with this ligand early reported.⁴⁰

Another structural property that can be analyzed for coordination bonds is the vibrational frequencies. The values of the vibrational frequencies $\nu(\text{NH}_2)$ and $\nu(\text{C}=\text{O})$ theoretically determined for the ligand were 1707 and 1740 cm $^{-1}$, respectively. The vibrational frequencies of the bonds decrease with coordination and the values found were 1679 cm $^{-1}$ for $\nu(\text{NH}_2)$ and 1722 cm $^{-1}$ for $\nu(\text{C}=\text{O})$. It is important to emphasize that no scale factor was used to correct the error associated

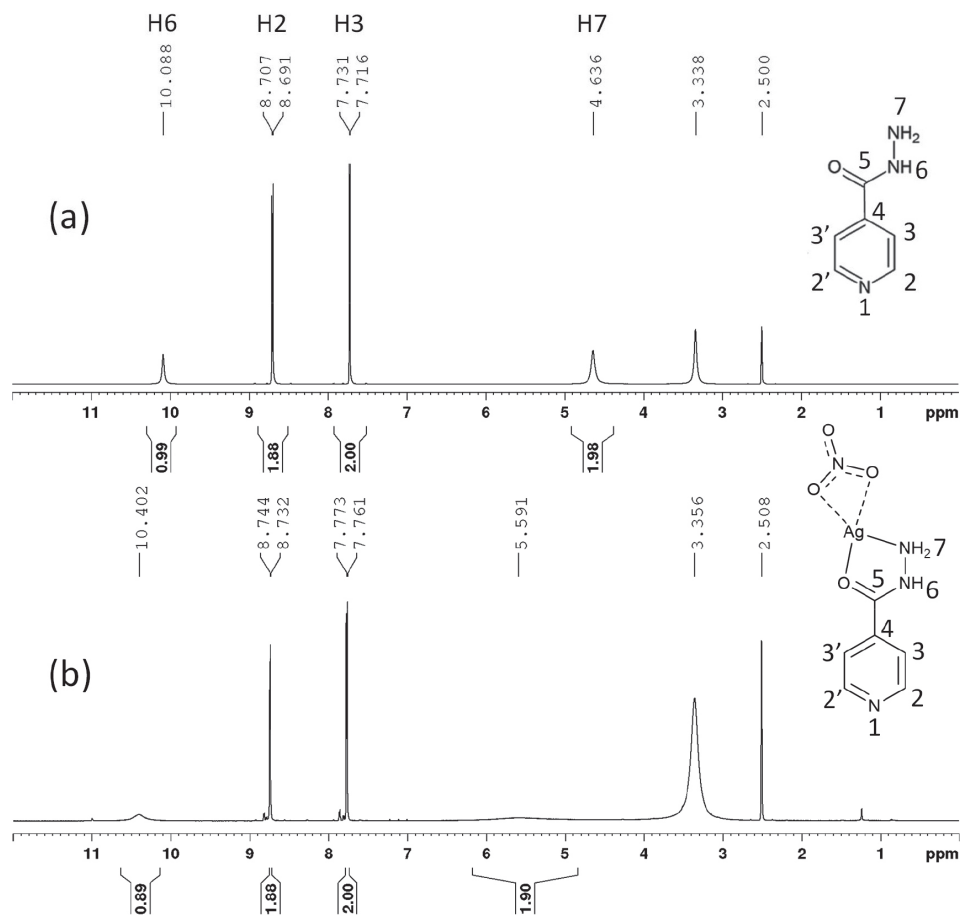


Figure 4. ^1H NMR spectra of (a) isoniazid and (b) silver complex

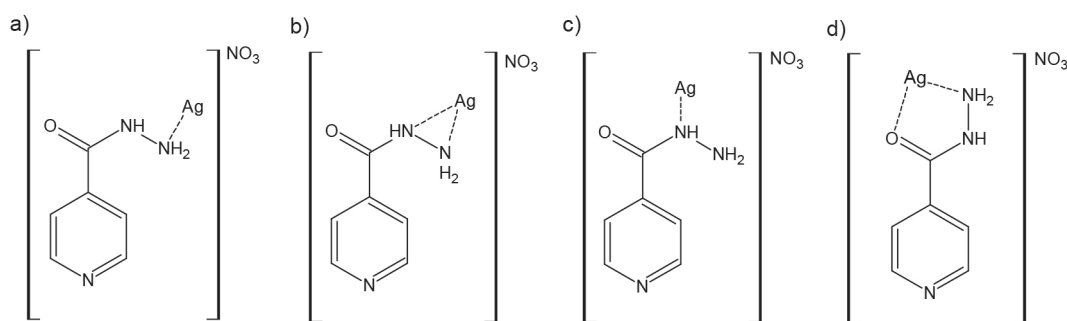


Figure 5. Simulated coordination modes of inh to Ag

with the calculation method, which justifies the difference in relation to the experimental data.

The QTAIM was used to better understand the electronic effects of the Ag-inh complex. In QTAIM analysis, the nature of the bond or interaction can be described by some parameters such as electronic density ($\rho(r)$), Laplacian of electronic density ($\nabla^2\rho(r)$), and total electronic energy ($H(r)$) ($H(r) = G(r) + V(r)$). According to QTAIM, values of $\nabla^2\rho(r) < 0$ indicate covalent bonds and $\nabla^2\rho(r) > 0$ indicate noncovalent bonds. When the values of $\nabla^2\rho(r)$ and $H(r)$ are positive, the nature of the interaction or bond is electrostatic, for $\nabla^2\rho(r)$ positive and $H(r)$ negative the bond are considered partially covalent.^{34,35}

The results for the QTAIM analysis for the Ag-N and Ag-O bonds are shown in Figure 6 along with the molecular graph of the complex. The values of $\nabla^2\rho(r)$ is positive and $H(r)$ is negative for the Ag-O bond showing that the bond has partially covalent character. For the Ag-N the values of $\nabla^2\rho(r)$ and $H(r)$ are positive showing that the bond has an electrostatic character.

Anti-Mycobacterium tuberculosis activity

The Ag-inh complex was active against *M. tuberculosis* with a MIC_{90} of $0.78 \pm 0.5 \mu\text{g mL}^{-1}$ ($2.55 \mu\text{mol L}^{-1}$). Although the Ag complex presents a MIC_{90} value higher than rifampicin ($0.08 \pm 0.02 \mu\text{g mL}^{-1}$) and inh itself ($0.13 \pm 0.06 \mu\text{g mL}^{-1}$ or $0.948 \mu\text{mol L}^{-1}$), it is lower than other antimycobacterial agents used in TB clinical treatments as ethambutol ($MIC_{90} = 5.62 \mu\text{g mL}^{-1}$) and p-aminosalicylic ($MIC_{90} = 1.25 \mu\text{g mL}^{-1}$). It is well established that free inh is a potent and selective prodrug that inhibits the biosynthesis of the mycobacteria

cell wall by interrupting the synthesis of mycolic acids. It is called a prodrug because it just becomes active after a transformation by a catalase-peroxidase enzyme, giving rise to isonicotinic acid.⁴¹ The rigidity and stability conferred to the complex by the silver atom could prevent the biotransformation of inh to isonicotinic acid and thus inhibit its activity but only additional studies could confirm or not this hypothesis. It was observed that the Ag-inh is active against *M. tuberculosis* and similar results were published in the literature with cobalt and copper complexes with isoniazid complexes, which have shown to be active against *M. tuberculosis* with MIC_{90} values of $0.41 \mu\text{mol L}^{-1}$ and $2.2 \mu\text{mol L}^{-1}$, respectively. Also, The MIC_{90} value was below the maximum limit of $25 \mu\text{g mL}^{-1}$, which is the value described in the literature that warrants for further studies of active compounds against *M. tuberculosis*. Montelongo-Peralta *et al.*²⁴ reported a study showing that an inh and Ag nitrate mixture, with no isolation of the complex, has a potent bactericidal effect on inh-resistant clinical *M. tuberculosis* strains, resulting in lower MIC values than those from the isolate components. However, the resulting MIC of AgNO_3 in the mixture was higher (around $10.0 \mu\text{mol L}^{-1}$) than that of the isolated Ag-isoniazid complex presented in this study ($2.55 \mu\text{mol L}^{-1}$).

Ahmed *et al.*⁴² studied the antimicrobial activity of a phenanthroline-isoniazid hybrid ligand (L) and its Ag^+ and Mn^{2+} complexes. The authors found that $[\text{Ag}(\text{L})_2]\text{BF}_4$, $[\text{Ag}(\text{L})_2]\text{NO}_3 \cdot 2\text{H}_2\text{O}$ and $[\text{Mn}(\text{L})_2](\text{-NO}_3)_2 \cdot 2\text{H}_2\text{O}$, were almost fourfold more potent than inh. Curiously, there was no real variation in activity across the group of metal complexes, suggesting that activity was independent of the type of chelated central metal ion (Ag^+ and Mn^{2+}).

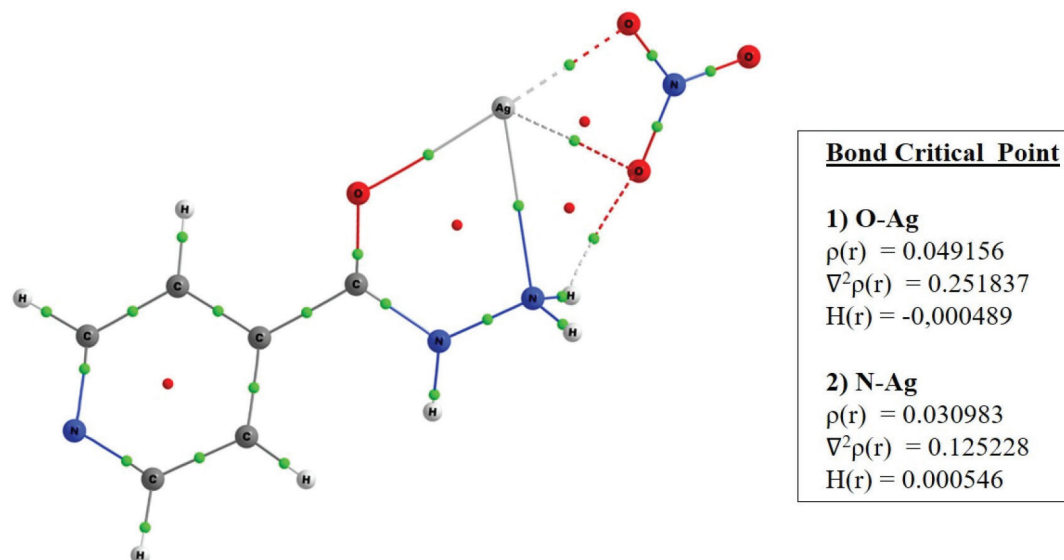


Figure 6. Molecular graph for $[\text{Ag}(\text{C}_6\text{H}_7\text{N}_3\text{O})]\text{NO}_3$ and topological parameter $\rho(r)$, $\nabla^2\rho(r)$ and $H(r)$ for Ag-N and Ag-O bonds generated by QTAIM. Bond critical points are represented by yellow circles, red circles are the ring critical points and the values of topological properties are in au

CONCLUSIONS

A new silver complex with isoniazid, with coordination formula $[Ag(C_6H_7N_3O)] \cdot NO_3$, was obtained. Infrared spectroscopic analysis permitted proposing coordination of the ligand to Ag by the N atom of the NH_2 group and oxygen atom of the C=O group. The 1H NMR spectroscopic measurements reinforced N coordination of NH_2 to the metal. The structures of inh and the Ag-inh complex were optimized to the minimum of energy using the density functional theory (DFT). The studies confirmed that the coordination mode where inh coordinates to Ag(I) by the nitrogen atom of NH_2 group and also by the O atom of C=O group is the most stable one. Bond lengths of $N \cdots Ag$ and $O \cdots Ag$ were 2.60 and 2.30 Å, respectively. The Ag-inh complex was active over *M. tuberculosis* with MIC_{90} of $0.78 \pm 0.5 \mu g mL^{-1}$ ($2.55 \mu mol L^{-1}$). Further analyses are envisaged to verify this hypothesis and ensure its potential as a drug candidate for the treatment of tuberculosis.

SUPPLEMENTARY MATERIAL

DSC and ^{13}C -NMR spectra for inh and the Ag complex are freely available at <http://quimicanova.sbq.org.br> in PDF format.

ACKNOWLEDGMENTS

This study was supported by grants from the Brazilian Agencies FAPESP (São Paulo State Research Council, Grants No. 2015/20882-3, 2017/11570-3 and 2018/12062-4). Douglas H. Pereira also acknowledges the Center for Computational Engineering and Sciences (Financial support from FAPESP, Grants No. 2013/08293-7 and 2017/11485-6) and the National Center for High Performance Processing (CENAPAD) in São Paulo for the computational resources. This study was partially financed by the Coordenação de Aperfeiçoamento de Pessoal de Nível Superior - Brasil (CAPES) – Finance Code 001.

REFERENCES

- WHO. *Global Tuberculosis Report 2019*, 2019, WHO: France.
- Cardoso, R. F.; Cooksey, R. C.; Morlock, G. P.; Barco, P.; Cecon, L.; Forestiero, F.; Leite, C. Q. F.; Sato, D. N.; Shikama, M. D.; Mamizuka, E. M.; Hirata, R. D. C.; Hirata, M. H.; *Antimicrob. Agents Chemother.* **2004**, *48*, 3373.
- Vaerewijck, M. J. M.; Huys, G.; Palomino, J. C.; Swings, J.; Portaels, F.; *FEMS Microbiol. Rev.* **2005**, *29*, 911.
- Domingos, S.; André, V.; Quaresma, S.; Martins, I. C. B.; Minas da Piedade, M. F.; Duarte, M. T.; *J. Pharm. Pharmacol.* **2015**, *67*, 830.
- Ames, J. R.; Ryan, M. D.; Kovacic, P.; *J. Free Radicals Biol. Med.* **1986**, *2*, 377.
- Sarkar, K.; Sen, K.; *Int. J. Pharm. Sci. Res.* **2015**, *6*, 1.
- Poggi, M.; Barroso, R.; Costa, A. J.; Barros, H. B.; Pavan, F. R.; Leite, C. Q.; Gambino, D.; Torre, M. H.; *J. Mex. Chem. Soc.* **2013**, *57*, 198.
- Freitas, M. C. R.; António, J. M. S.; Zioli, R. L.; Yoshida, M. I.; Rey, N. A.; Diniz, R.; *Polyhedron* **2011**, *30*, 1922.
- Almeida, F. B.; Cunha, M. S.; Abreu, H. A.; Diniz, R.; *ChemistrySelect* **2016**, *1*, 3770.
- Almeida, F. B.; Silva, F. H.; Abreu, H. A.; Diniz, R.; *J. Coord. Chem.* **2015**, *68*, 1282.
- de Gracia, C. G.; *Burns* **2001**, *27*, 67.
- Klasen, H. J.; *Burns* **2000**, *26*, 131.
- Nomiya, K.; Yokoyama, H.; *J. Chem. Soc., Dalton Trans.* **2002**, *12*, 2483.
- Nomiya, K.; Kondoh, Y.; Onoue, K.; Kasuga, N. C.; Nagano, H.; Oda, M.; Sudoh, T.; Sakuma, S.; *J. Inorg. Biochem.* **1995**, *58*, 255.
- Mjos, K. D.; Orvig, C.; *Chem. Rev. (Washington, DC, U. S.)* **2014**, *114*, 4540.
- Berners-Price, S. J.; Johnson, R. K.; Giovenella, A. J.; Faucette, L. F.; Mirabelli, C. K.; Sadler, P. J.; *J. Inorg. Biochem.* **1988**, *33*, 285.
- Klasen, H. J.; *Burns* **2000**, *26*, 117.
- Nomiya, K.; Noguchi, R.; Oda, M.; *Inorg. Chim. Acta* **2000**, *298*, 24.
- Nomiya, K.; Noguchi, R.; Shigetani, T.; Kondoh, Y.; Tsuda, K.; Ohsawa, K.; Chikaraishi-Kasuga, N.; Oda, M.; *Bull. Chem. Soc. Jpn.* **2000**, *73*, 1143.
- Wang, H.; Wang, M.; Yang, X.; Xu, X.; Hao, Q.; Yan, A.; Hu, M.; Lobinski, R.; Li, H.; Sun, H.; *Chem. Sci.* **2019**, *10*, 7193.
- Wang, H.; Yan, A.; Liu, Z.; Yang, X.; Xu, Z.; Wang, Y.; Wang, R.; Koochi-Moghadam, M.; Hu, L.; Xia, W.; Tang, H.; Wang, Y.; Li, H.; Sun, H.; *PLoS Biol.* **2019**, *17*, e3000292.
- Matsui, Y.; Otomo, K.; Ishida, S.; Yanagihara, K.; Kawanobe, Y.; Kida, S.; Taruoka, E.; Sugawara, I.; *Microbiol. Immunol.* **2004**, *48*, 489.
- Manzano, C. M.; Nakahata, D. H.; Tenorio, J. C.; Lustrí, W. R.; Resende Nogueira, F. A.; Aleixo, N. A.; da Silva Gomes, P. S.; Pavan, F. R.; Grecco, J. A.; Ribeiro, C. M.; Corbi, P. P.; *Inorg. Chim. Acta* **2020**, *502*, 119293.
- Montalongo-Peralta, L. Z.; León-Buitimea, A.; Palma-Nicolás, J. P.; Gonzalez-Christen, J.; Morones-Ramírez, J. R.; *Sci. Rep.* **2019**, *9*, 5471.
- Palomino, J.-C.; Martin, A.; Camacho, M.; Guerra, H.; Swings, J.; Portaels, F.; *Antimicrob. Agents Chemother.* **2002**, *46*, 2720.
- Becke, A. D.; *J. Chem. Phys.* **1993**, *98*, 5648.
- Lee, C.; Yang, W.; Parr, R. G.; *Phys. Rev. B* **1988**, *37*, 785.
- Vosko, S. H.; Wilk, L.; Nusair, M.; *Can. J. Phys.* **1980**, *58*, 1200.
- Ditchfield, R.; Hehre, W. J.; Pople, J. A.; *J. Chem. Phys.* **1971**, *54*, 724.
- Hehre, W. J.; Ditchfield, R.; Pople, J. A.; *J. Chem. Phys.* **1972**, *56*, 2257.
- Hariharan, P. C.; Pople, J. A.; *Theor. Chim. Acta* **1973**, *28*, 213.
- Hay, P. J.; Wadt, W. R.; *J. Chem. Phys.* **1985**, *82*, 270.
- Frisch, J.; Trucks, G. W.; Schlegel, H. B.; Scuseria, G. E.; Robb, M. A.; Cheeseman, J. R.; Scalmani, G.; Barone, V.; Mennucci, B.; Petersson, G. A.; Nakatsuji, H.; Caricato, M.; Li, X.; Hratchian, H. P.; Izmaylov, A. F.; Bloino, J.; Zheng, G.; Sonnenberg, J. L.; Hada, M.; Ehara, M.; Toyota, K.; Fukuda, R.; Hasegawa, J.; Ishida, M.; Nakajima, T.; Honda, Y.; Kitao, O.; Nakai, H.; Vreven, T.; Montgomery, J. A.; Peralta, J. E.; Ogliaro, F.; Bearpark, M.; Heyd, J. J.; Brothers, E.; Kudin, K. N.; Staroverov, V. N.; Kobayashi, R.; Normand, J.; Raghavachari, K.; Rendell, A.; Burant, J. C.; Iyengar, S. S.; Tomasi, S.; Cossi, M.; Rega, N.; Millam, J. M.; Klene, M.; Knox, J. E.; Cross, J. B.; Bakken, V.; Adamo, C.; Jaramillo, J.; Gomperts, R.; Stratmann, R. E.; Yazyev, O.; Austin, A. J.; Cammi, R.; Pomelli, C.; Ochterski, J. W.; Martin, R. L.; Morokuma, K.; Zakrzewski, V. G.; Voth, G. A.; Salvador, P.; Dannenberg, J. J.; Dapprich, S.; Daniels, A. D.; Farkas, Ö.; Foresman, J. B.; Ortiz, J. V.; Cioslowski, J.; Fox, D. J.; *Gaussian 09, Revision D.1*; Gaussian, Inc., Wallingford CT, 2016.
- Bader, R. F. W.; *Atoms in molecules: a quantum theory*, 1st ed., Clarendon Press: Wotton-under-Edge, 1994.
- Ribeiro, I.; Reis, D.; Pereira, D.; *J. Mol. Model.* **2019**, *25*, 267.
- Keith, T.A.; *AIMAll (Version 17.11.14)*; Overland Park, USA, 2017.
- Borba, A.; Gómez-Zavaglia, A.; Fausto, R.; *J. Chem. Phys. A* **2009**, *113*, 9220.
- Nakamoto, K.; *Infrared and Raman spectra of inorganic and coordination compounds*, 5th ed., Wiley: New York, 1997.
- Goebbert, D. J.; Garand, E.; Wende, T.; Bergmann, R.; Meijer, G.; Asmis, K. R.; Neumark, D. M.; *J. Phys. Chem. A* **2009**, *113*, 7584.
- Hanson, J. C.; Camerman, N.; Camerman, A.; *J. Med. Chem.* **1981**, *24*, 1369.
- Oliveira, J.; Sousa, E.; Basso, L.; Palaci, M.; Dietze, R.; Santos, D.; Moreira, I.; *Chem. Commun.* **2004**, *10*, 312.
- Ahmed, M.; Rooney, D.; McCann, M.; Devereux, M.; Twamley, B.; Galdino, A. C. M.; Sanganito, L. S.; Souza, L. O. P.; Lourenço, M. C.; Gomes, K.; Santos, A. L. S.; *BioMetals* **2019**, *32*, 671.

